

# Impact of Pilot-Scale Rolling and Heat Treatment on the Toughness of CrNiMoV Steel Plates

M.F. Buchely <sup>1\*</sup>, R. Cardoso <sup>2</sup>, L. Bartlett <sup>1</sup>, R. O'Malley <sup>1</sup>, D. Field <sup>3</sup>, K. Limmer <sup>3</sup>

<sup>1</sup> Missouri University of Science and Technology, Department of Materials Science and Engineering  
1400N. Bishop, Rolla, MO 65409, USA.

<sup>2</sup> Nucor-Yamato Steel Company, 5929 AR-18  
Blytheville, AR 72315, USA.

<sup>3</sup> U.S. Army Combat Capabilities Development Command Army Research Laboratory  
6300 Rodman Rd., Aberdeen Proving Ground, MD 21005, USA.

\*Corresponding to author: email: buchelym@mst.edu; (573) 341-6972

## ABSTRACT

The thermomechanical processing of CrNiMoV steels presents significant challenges due to their complex alloy composition and the need to achieve an optimal balance between hardness and toughness. In this study, a CrNiMoV steel slab, industrially produced at 8 inches thick, was hot rolled to a final plate thickness of 1.5 inches using a pilot-scale rolling mill with a capacity of 4.5 metric Tons. The rolling trials were designed to simulate industrial rolling practices while exploring the effect of deformation on microstructural evolution. A dilatometry study was performed to investigate phase transformations under varying cooling rates, providing insights into critical phase changes during processing. After rolling, the plates were subjected to a comprehensive heat treatment cycle, including normalization, subcritical annealing, quenching, and tempering, to achieve maximum mechanical performance. The processed plates were then compared to an industrially produced 1-inch-thick plate from the same steel batch. The microstructure evolution was analyzed at different stages of the heat treatment cycle, and Charpy impact tests were conducted to evaluate toughness in both the as-rolled and heat-treated conditions. The results highlight the significant influence of rolling thickness reduction on microstructure refinement and toughness improvement. This study provides critical insights into the relationship between rolling practices, phase transformations, and mechanical properties in CrNiMoV steels, aiming to optimize controlled rolling strategies for industrial production of thick plates.

Keywords: CrNiMoV steel, Thermomechanical processing, Charpy impact test, Microstructure evolution.

## INTRODUCTION

High-performance structural steels are essential in demanding applications such as military vehicles, tooling, mining equipment, and heavy-duty machinery, where a reliable combination of high strength, hardness, and toughness is required [1]. Among these, CrNiMoV steels are widely used due to their excellent hardenability and mechanical properties, which stem from their alloying elements and heat treatment response [2]. However, achieving an optimal balance between strength and toughness remains a challenge, particularly in thick sections, where heterogeneous microstructures and residual stresses can compromise performance [3].

Conventional processing of these steels often involves a quench and temper (Q&T) cycle applied to as-cast or standard plate materials [4]. While effective, this approach may not fully utilize the microstructural refinement opportunities available through thermomechanical processing strategies such as controlled rolling [5]. Controlled rolling, especially when partially conducted below the recrystallization temperature ( $T_R$ ), can refine the prior austenite grain structure, enhance hardenability, and improve final mechanical performance [6]. Nevertheless, limited studies have explored how these process variables impact subsequent transformations and property evolution in CrNiMoV steels, particularly in industrially relevant thicknesses.

This study investigates the influence of a controlled hot rolling schedule on the microstructure evolution and mechanical properties of a CrNiMoV steel plate, in comparison to a reference plate subjected to conventional Q&T processing. The rolling schedule was designed with 80% of the total deformation above  $T_R$ , and the final 20% below  $T_R$  to deform austenite under non-recrystallized conditions and encourage the development of finer martensitic packets upon transformation. This approach aims to enhance the impact toughness without compromising hardness.

To assess the effects of this thermomechanical treatment, the rolled plate and the reference plate were both subjected to a full laboratory heat treatment cycle, including normalizing, subcritical annealing, quenching, and tempering. Dilatometry studies, supported by JMatPro simulations, were used to develop continuous cooling transformation (CCT) diagrams and understand the transformation behavior of the plates at different cooling rates. Microstructural characterization using scanning electron microscopy (SEM), along with hardness and Charpy V-Notch (CVN) impact testing at  $-40\text{ }^{\circ}\text{C}$ , was employed to evaluate the microstructural evolution and mechanical performance.

The findings reveal that controlled rolling, combined with post-processing heat treatment, produces a favorable martensite microstructure with improved toughness compared to the conventionally processed reference plate. These improvements are attributed to refined prior austenite grains and enhanced transformation kinetics, highlighting the potential of controlled thermomechanical processing routes to optimize the performance of high-strength, high-toughness steels for critical structural applications.

## MATERIALS AND METHODS

The chemical composition of the CrNiMoV steel studied in this work is shown in Table 1. Figure 1 presents the JMatPro predictions for this alloy, including equilibrium phase formation and the corresponding continuous cooling transformation (CCT) behavior, which were used to support the interpretation of thermal processing and microstructural evolution.

The material was industrially produced via continuous casting and partially rolled into 8-inch-thick slabs. These slabs were cut into smaller blocks using oxy-fuel torch cutting, as illustrated in Figure 2a. One of the blocks was machined to eliminate surface defects and the heat-affected zone from cutting, resulting in a final block of dimensions  $8'' \times 6'' \times 10''$ , which was used for pilot-scale rolling trials, as schematically shown in Figure 2b.

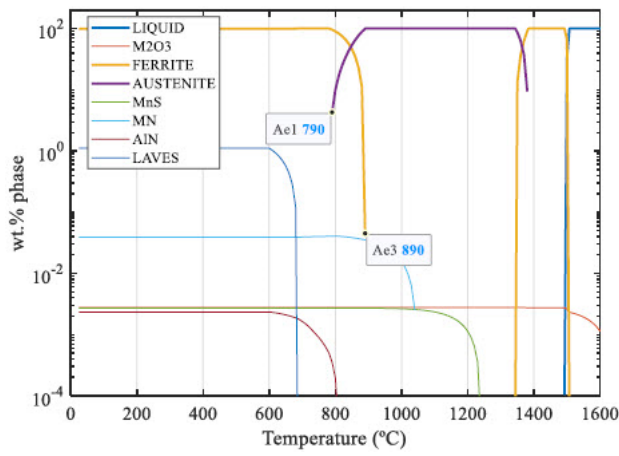
Rolling was performed using a pilot-scale reversible rolling mill with a capacity of 4.5 metric tons. The block was reheated to  $1250\text{ }^{\circ}\text{C}$  for 4 hours, followed by 8 rolling passes. The first five passes were conducted above the recrystallization temperature ( $T_R \approx 975\text{ }^{\circ}\text{C}$ ), reducing thickness from 8'' to 2''. The final three passes were carried out below  $T_R$  to 1'' to promote controlled microstructure refinement. Surface temperature was monitored using single-color pyrometers positioned at the entry and exit side of the mill. After rolling, the plate was slow-cooled in vermiculite to minimize cracking risk due to its high alloy content. This material is referred to hereafter as the *rolled plate*.

For comparison, an industrially produced plate with the same chemical composition was also characterized. This reference plate (*ref. plate*) was cross-hot rolled to a final thickness of 1 inch, then austenitized at  $913\text{ }^{\circ}\text{C}$  for 25 minutes, quenched in water, and tempered at  $205\text{ }^{\circ}\text{C}$  for 56 minutes. The full rolling schedule for the ref. plate was not available.

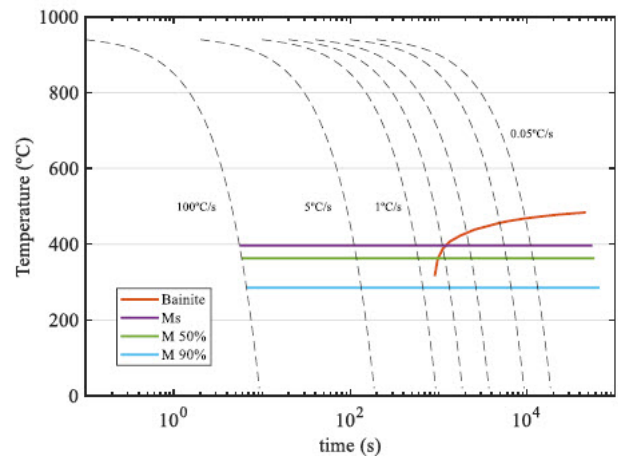
Following rolling, the rolled plate and ref. plate underwent a comprehensive heat treatment sequence to enhance toughness and strength, consisting of: hydrogen bake, normalization, subcritical annealing, quenching, and tempering, as shown schematically in Figure 3.

Table 1. Chemical composition of the CrNiMoV steel alloy (wt.%). Fe in balance.

C	Mn	Si	Cr	Ni	Mo	V	N, ppm	Al	S, ppm	P, ppm	Cu	O, ppm
0.29	0.69	1.0	2.71	0.98	0.94	0.1	82	0.008	10	60	0.17	13



(a)

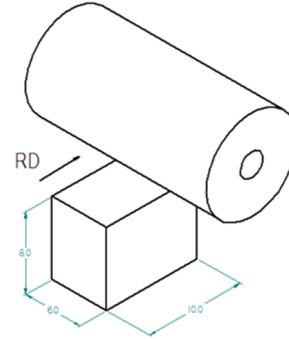


(b)

Figure 1. JMatPro simulations for the studied CrNiMoV steel alloy: (a) Predicted equilibrium phase diagram indicating critical transformation temperatures Ae1 (austenite finish) and Ae3 (ferrite start); (b) Continuous Cooling Transformation (CCT) diagram showing phase evolution under various cooling rates, including 100, 5, 1, 0.5, 0.25, 0.1, and 0.05 °C/s.



(a)



(b)

Figure 2. CrNiMoV steel alloy used in this study: (a) Partially rolled slab as received from the continuous casting process, and (b) schematic showing slab orientation and rolling direction during hot rolling (dimensions in inches).

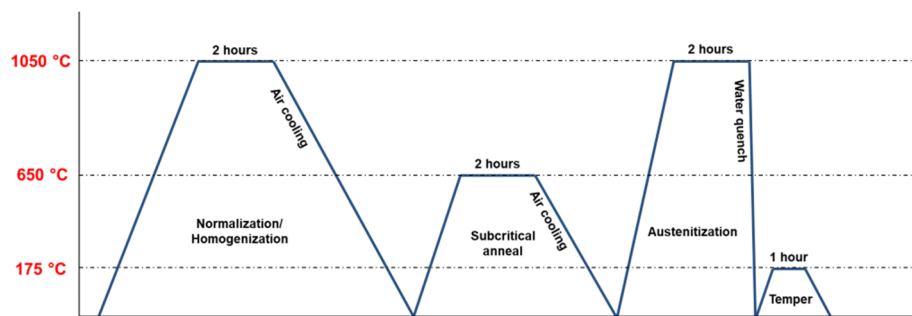


Figure 3. Schematic of the heat treatment cycle applied to the rolled and reference plates. Note: the hydrogen baking step is not included in the diagram.

Characterization included microstructural analysis via scanning electron microscopy (SEM), hardness testing using the Rockwell C scale, and Charpy V-notch (CVN) impact testing at  $-40$  °C in both longitudinal (LT) and transverse (TL) directions relative to the rolling direction.

A dilatometry study was also conducted using a RITA Linseis quenching/deformation dilatometer to investigate the hardenability and phase transformation behavior under various cooling rates. Samples with dimensions 3 mm diameter  $\times$  10 mm length were machined from the rolled plate and ref. plate, austenitized at 1200 °C for 3 minutes, and cooled under controlled conditions.

## RESULTS AND DISCUSSION

### Thermomechanical Processing via Pilot-Scale Rolling

Figure 4 presents the recorded data from the rolling schedule applied to the studied material. Figure 4a shows the rolling force profile across the eight passes, while Figure 4b displays the surface temperature measured during the hot rolling process. The first five passes were conducted above  $T_R$  ( $>975^{\circ}\text{C}$ ), although pyrometer readings indicated lower surface temperatures than expected based on the initial slab reheat temperature of  $1250^{\circ}\text{C}$ . This discrepancy is likely due to the formation of a relatively thick oxide scale after reheating, which interfered with the accuracy of the optical pyrometer during early passes. Following mechanical removal of this oxide layer during the initial deformation, the subsequent temperature readings appear to be more accurate. During the first five passes, rolling forces remained below  $1.75\text{ MN}$ , well within the capacity of the rolling mill (maximum  $4.5\text{ MN}$ ).

Following the fifth pass, the slab was held for approximately 150 seconds to allow its surface temperature to drop below  $T_R$ , as shown in Figure 4b. The final three passes were carried out in this lower temperature regime to promote deformation of the austenitic grains, which contributes to microstructural refinement. This approach is intended to generate finer martensitic packets upon transformation, ultimately enhancing the strength and toughness of the final material. Table 2 summarizes the rolling schedule applied to the studied alloy.

Figure 5 shows the rolled plate following slow cooling under vermiculite insulation. The final plate dimensions were approximately 1.4 inches in thickness and 7.5 inches in width. The target thickness of 1 inch was not fully achieved due to incomplete engagement of the rolling mill during the final pass, as evidenced by the reduced rolling force in this stage (see last pass force in Figure 4a).

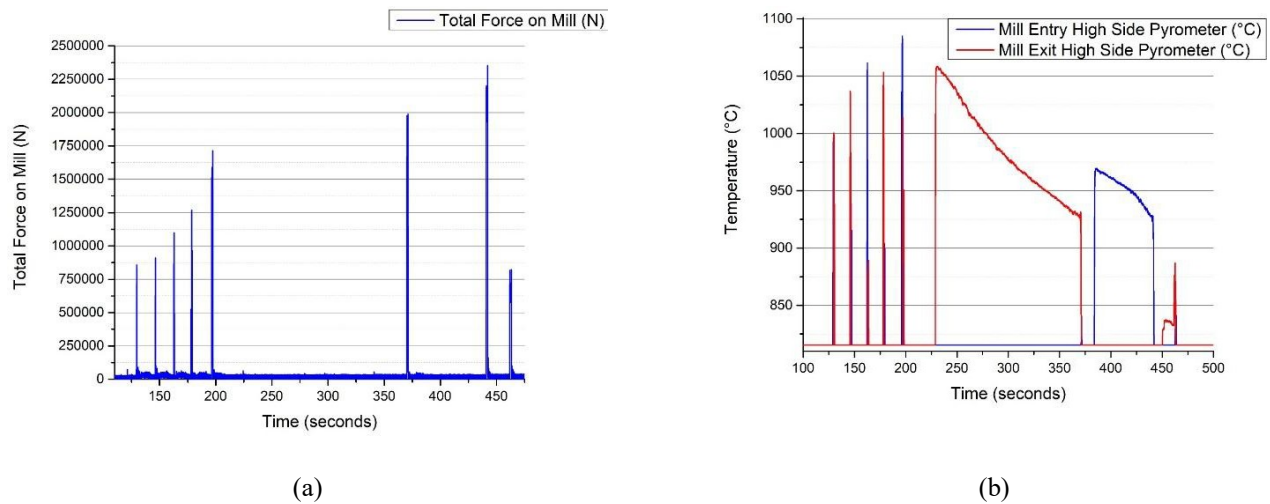


Figure 4. Hot rolling schedule results for the CrNiMoV steel: (a) Rolling force profile (in N) across eight reduction passes, and (b) surface temperature history (in  $^{\circ}\text{C}$ ) recorded by entry and exit pyrometers on the reversible rolling mill.

Table 2. Hot rolling schedule designed for the studied CrNiMoV steel: 80% of total reduction passes conducted above the recrystallization temperature  $T_R$ , and 20% conducted below  $T_R$  to refine the austenitic grain structure.

Pass #	Theoretical reduction (%)	Measured force max. [kN]	Measured temperature [ $^{\circ}\text{C}$ ]	
			(min)	(max)
1	13.9	870		1003
2	16.8	944		1040
3	20.8	1142		1067
4	26.1	1329		1058

5	32.3	1799		1093
6	20	2238	947	1067
7	21.9	2672	951	988
8	20	1154	860	912

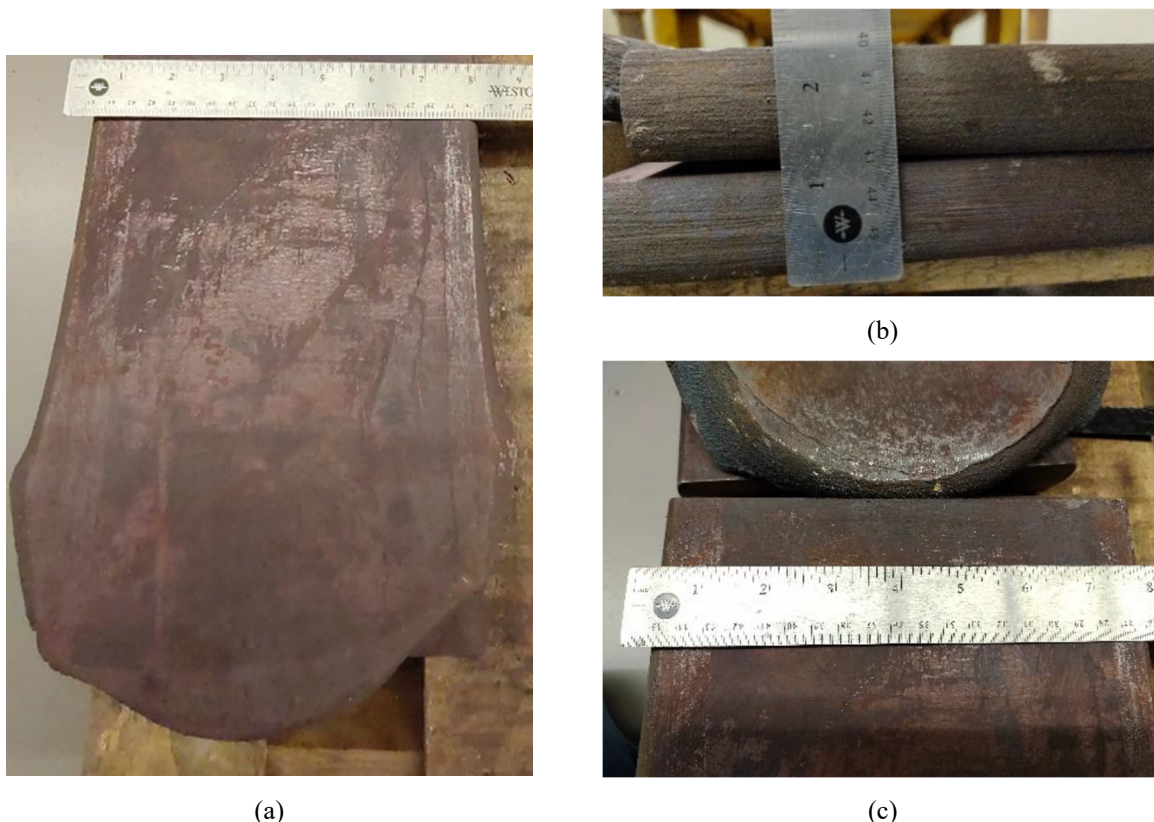


Figure 5. Rolled CrNiMoV steel plate after hot rolling and slow cooling under vermiculite. Final dimensions: 1.4” thickness and 7.5” width: (a) top view, (b) side view, and (c) details of the plate width.

#### Dilatometric Characterization of CrNiMoV Steel

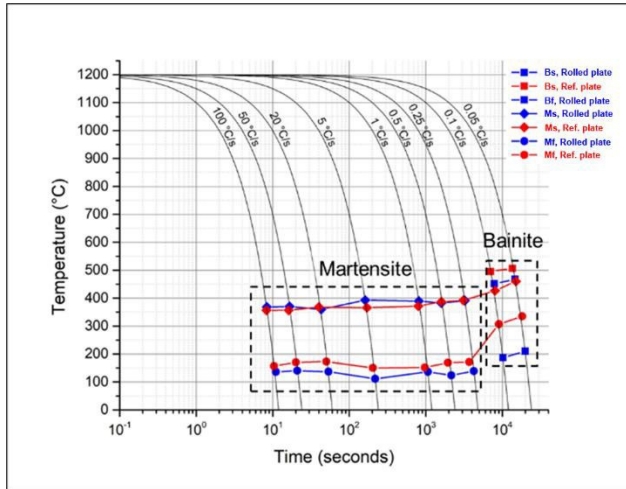
Figure 6 presents the results of the dilatometry study, including the continuous cooling transformation (CCT) diagrams for both the rolled and reference plates, as well as selected SEM micrographs of the rolled plate after cooling at various rates during the dilatometric cycles.

From the CCT diagrams, it can be observed that the martensite start ( $M_s$ ) temperature is nearly identical for both plates, occurring at approximately 380 °C. In contrast, the martensite finish ( $M_f$ ) temperature is slightly higher for the reference plate, while the rolled plate completes its transformation around 110 °C. Both materials exhibit full martensitic transformation at medium to low cooling rates, down to 0.25 °C/s, indicating the high hardenability of this CrNiMoV alloy. This suggests that even relatively air cooling can still result in a predominantly martensitic structure. When compared to the JMatPro predictions Figure 1a, the  $M_s$  temperature is in good agreement, predicted at 395 °C versus the experimentally observed 380 °C. However, the  $M_f$  temperature shows a notable discrepancy. JMatPro suggests only 90% martensitic transformation occurring around 330 °C, which contrasts with the experimental dilatometry results indicating a much lower  $M_f$  temperature near 120 °C. This deviation highlights limitations in equilibrium-based modeling tools when applied to complex, high-hardenability steels under non-equilibrium cooling conditions.

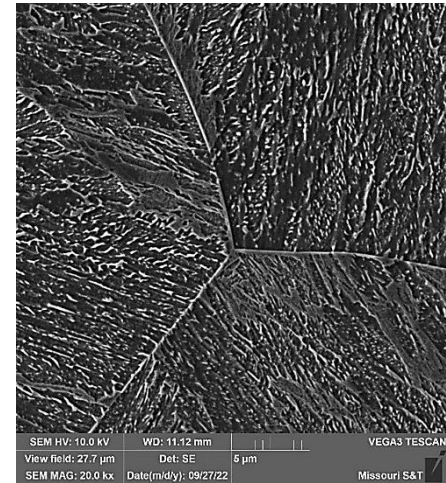
At lower cooling rates of 0.05 °C/s and 0.1 °C/s, partial bainitic transformation was experimentally detected in both plates. Notably, the reference plate exhibited a higher fraction of bainite, which could be attributed to a coarser prior austenite grain size. In contrast, the rolled plate underwent controlled rolling below the recrystallization temperature, likely producing finer



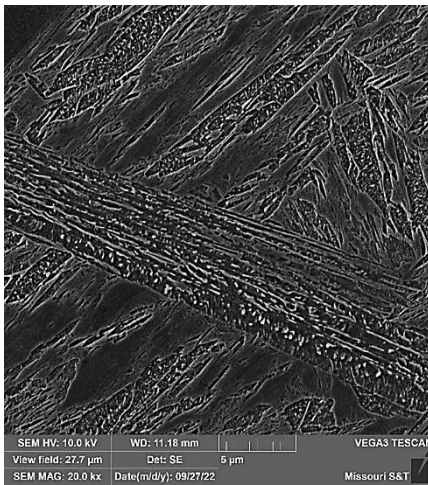
austenitic grains. These finer grains may have recrystallized more effectively during the dilatometric reheating, thus enhancing the hardenability and favoring martensite formation over bainite. When compared to the JMatPro predictions, the model suggests bainite formation occurs at cooling rates as high as 0.5 °C/s, whereas the experimental results indicate bainite appears only at slower rates, such as 0.25 °C/s or below. This discrepancy can be attributed to differences in segregation behavior and prior austenite grain size, which are not fully captured in equilibrium-based simulation tools.



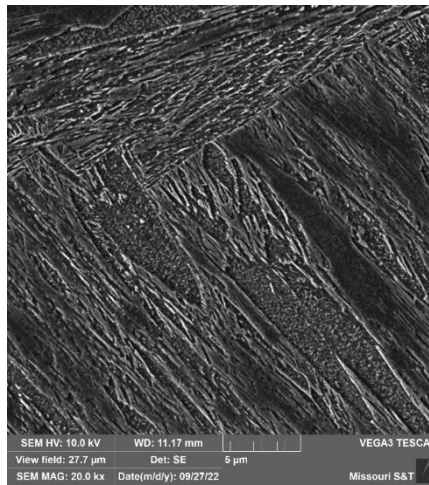
(a)



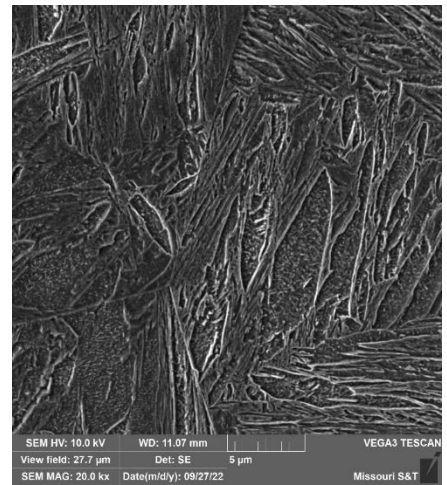
(b)



(c)



(d)



(e)

Figure 6. Dilatometry results: (a) Continuous Cooling Transformation Diagram and comparison between rolled material and reference plate after dilatometry studies at different cooling rates: (b) 0.05 °C/s, (c) 0.1 °C/s, (d) 0.25 °C/s and (e) 0.5 °C/s.

The microstructural evaluation of the rolled plate reveals a predominantly bainitic matrix at a cooling rate of 0.05 °C/s (Figure 6b). At 0.1 °C/s, a mixture of bainite and untempered martensite is evident (Figure 6c). With increasing cooling rates, martensite becomes dominant: at 0.25–0.5 °C/s, the structure transitions to fully martensitic, featuring both auto-tempered and untempered martensite plates (Figure 6d-e). The presence of auto-tempered martensite suggests that, due to the alloy high hardenability, transformation occurs at relatively high  $M_s$  temperatures and under cooling rates slow enough to permit partial tempering during cooling. This effect is consistent with longer exposure near the temperature ranges associated with Stage 2 and Stage 3 tempering, allowing for diffusion-driven tempering mechanisms to operate during transformation.

## Heat Treatment, Microstructure Evolution and Impact Toughness

Figure 7 presents the microstructures of the plates prior to heat treatment. For the rolled plate (Figure 7a), the microstructure is primarily composed of bainite with a granular morphology, along with localized regions of untempered martensite. The average hardness of this condition was measured at 39 HRC. Given that the plate was slow-cooled in vermiculite, this mixed microstructure is consistent with expectations. Based on the CCT diagram developed for this alloy (Figure 6a) and the observed phases, the estimated cooling rate during slow cooling was between 0.05 and 0.1 °C/s.

In contrast, the reference plate (Figure 7b) exhibits a predominantly martensitic microstructure, with an average hardness of 54 HRC, close to the maximum expected for the carbon content of this steel. This result aligns with the known industrial heat treatment cycle applied to the reference plate: water quenching and tempering at 205 °C for 56 minutes. The observed fully martensitic microstructure is consistent with this thermal cycle.

Figure 8 illustrates the microstructural evolution of the rolled plate throughout the heat treatment sequence, along with the corresponding average hardness values. After the normalization step (Figure 8a), the microstructure consists of a bainitic matrix with regions of untempered martensite. This condition is consistent with a cooling rate of approximately 0.1 °C/s, typical of air cooling. The hardness at this stage was measured at 41.6 HRC, reflecting the mixed bainitic-martensitic structure. Following subcritical annealing (Figure 8b), the microstructure exhibits a more granular appearance. This morphology results from carbon partitioning within the bainite and partial tempering of untempered martensite, leading to a reduced hardness of 24.4 HRC. After quenching (Figure 8c), the matrix transforms into fully martensitic, with clear evidence of auto-tempered martensite, as previously discussed. The average hardness increased to 49.8 HRC at this stage. The final tempering step (Figure 8d) retains the overall martensitic morphology, now fully tempered, with a slight drop in hardness to 48.5 HRC. This microstructural refinement and controlled tempering are essential for balancing strength and toughness in the final material.

Figure 8e presents the Charpy V-Notch (CVN) impact toughness results for the rolled plate, both in the as-rolled condition and after the full heat treatment cycle. The results indicate a degree of toughness anisotropy, with the transverse-longitudinal (TL) direction showing approximately 20% lower toughness compared to the longitudinal-transverse (LT) direction, attributed to the rolling-induced texture. In the as-rolled condition, the plate exhibited an average impact energy of ~17 J, consistent with its mixed microstructure of bainite and untempered martensite, which typically results in reduced toughness. After heat treatment, the toughness significantly improved, reaching an average of 36 J at -40 °C. This value is considered above the standards for a martensitic microstructure and highlights the effectiveness of the heat treatment in enhancing low-temperature impact resistance.

Similarly, Figure 9 shows the microstructural evolution and CVN toughness of the reference plate through heat treatment. Similar phases to the rolled plate were observed, including bainite–martensite mixtures after normalization (Figure 9a) and annealing (Figure 9b), followed by auto-tempered and untempered martensite after quenching (Figure 9c), and fully tempered martensite after tempering (Figure 9d).

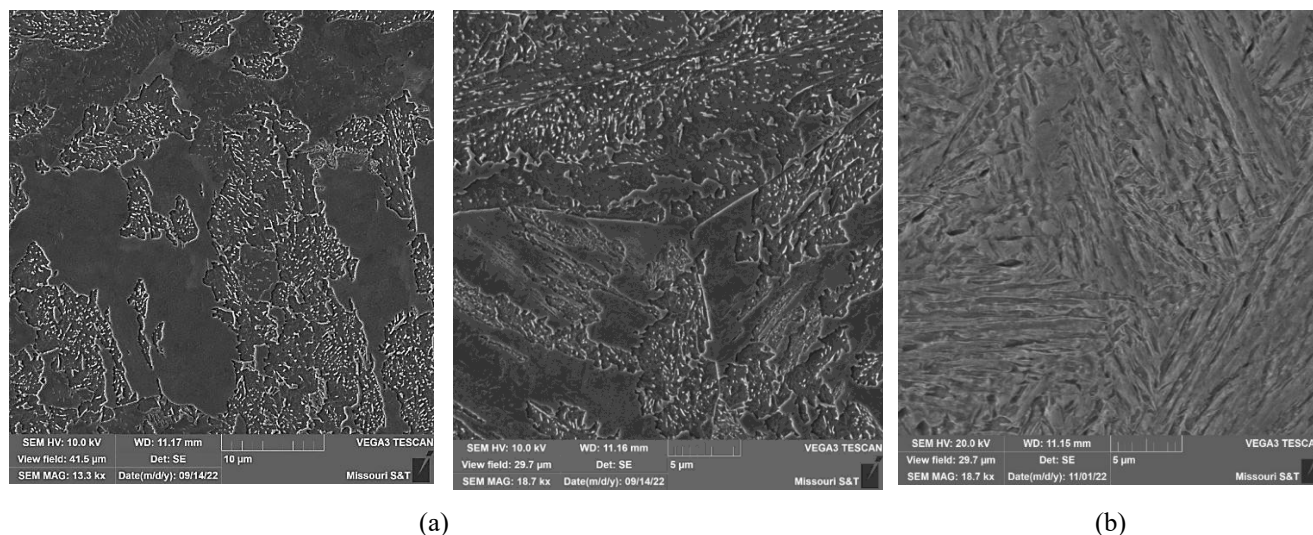
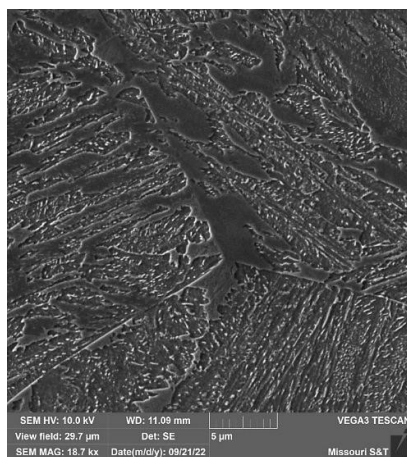
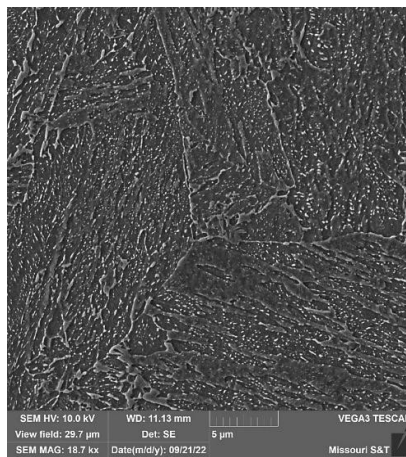


Figure 7. Microstructures before heat treatment: (a) rolled plate: 39 HRC, and (b) ref. plate: 54HRC.

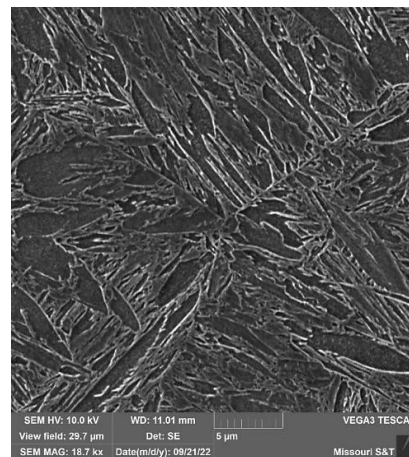




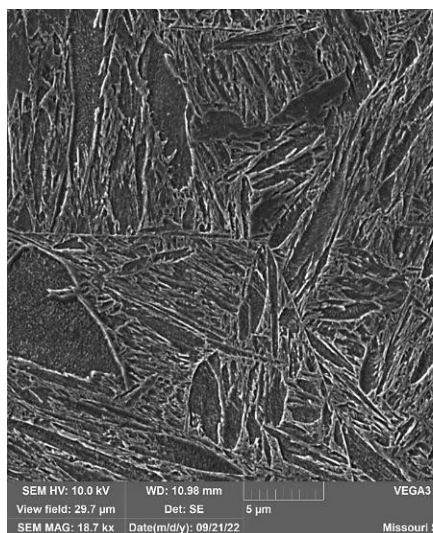
(a) After Normalization:  $41.67 \pm 0.50$  HRC



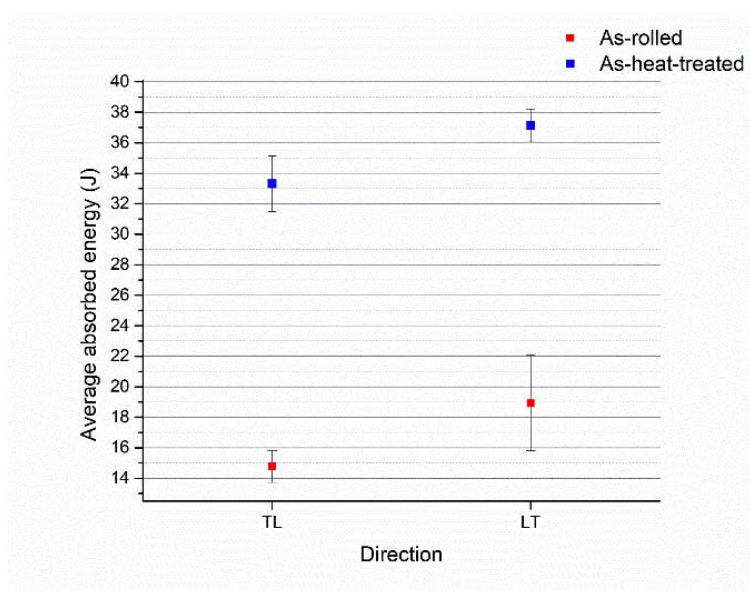
(b) After Subcritical annealing:  $24.45 \pm 0.75$  HRC.



(c) After Quenching:  $49.82 \pm 0.79$  HRC.



(d) After tempering:  $48.54 \pm 0.32$  HRC.



(e)

Figure 8. Rolled plate results: (a)-(d): Microstructural evolution throughout the heat treatment sequence, along with the corresponding average hardness values. (e) Impact toughness results from the CVN testing in both directions Longitudinal (LT) and Transverse (TL), and in the as-rolled and after heat treatment condition.

However, the reference plate exhibited a higher hardness (35 HRC) after subcritical annealing compared to the rolled plate (24 HRC). This difference may be due to the rolled plate containing more untempered martensite and retained austenite after normalization, which likely transformed to softer ferrite during annealing. In contrast, the reference plate had more bainite, which tempered but retained higher hardness. This effect likely contributed to the higher final hardness of the reference plate after tempering, which reached 51 HRC, compared to 48 HRC for the rolled plate. The greater bainite fraction in the reference plate, combined with its reduced softening during subcritical annealing, resulted in a harder tempered martensitic structure.

Now, Figure 9e presents the Charpy V-Notch (CVN) impact toughness results for the reference plate. Prior to the full heat treatment, the reference plate, already industrially quenched and tempered, exhibited high toughness values around 37 J. No noticeable anisotropy was observed, likely due to the cross-rolling practice used during its production. However, after undergoing the full laboratory heat treatment, the plate exhibited the typical toughness anisotropy associated with continuously casting/rolling, directionally rolled plates.



Notably, the rolled plate (Figure 8e) showed slightly higher toughness, by approximately 2–3 J, compared to the reference plate (Figure 9e). While this difference may seem marginal, it can be critical for applications where impact or abrasion resistance determines pass/fail criteria in performance testing. These results suggest that the controlled rolling strategy applied to the rolled plate can offer a more favorable hardness–toughness balance for this CrNiMoV steel alloy.

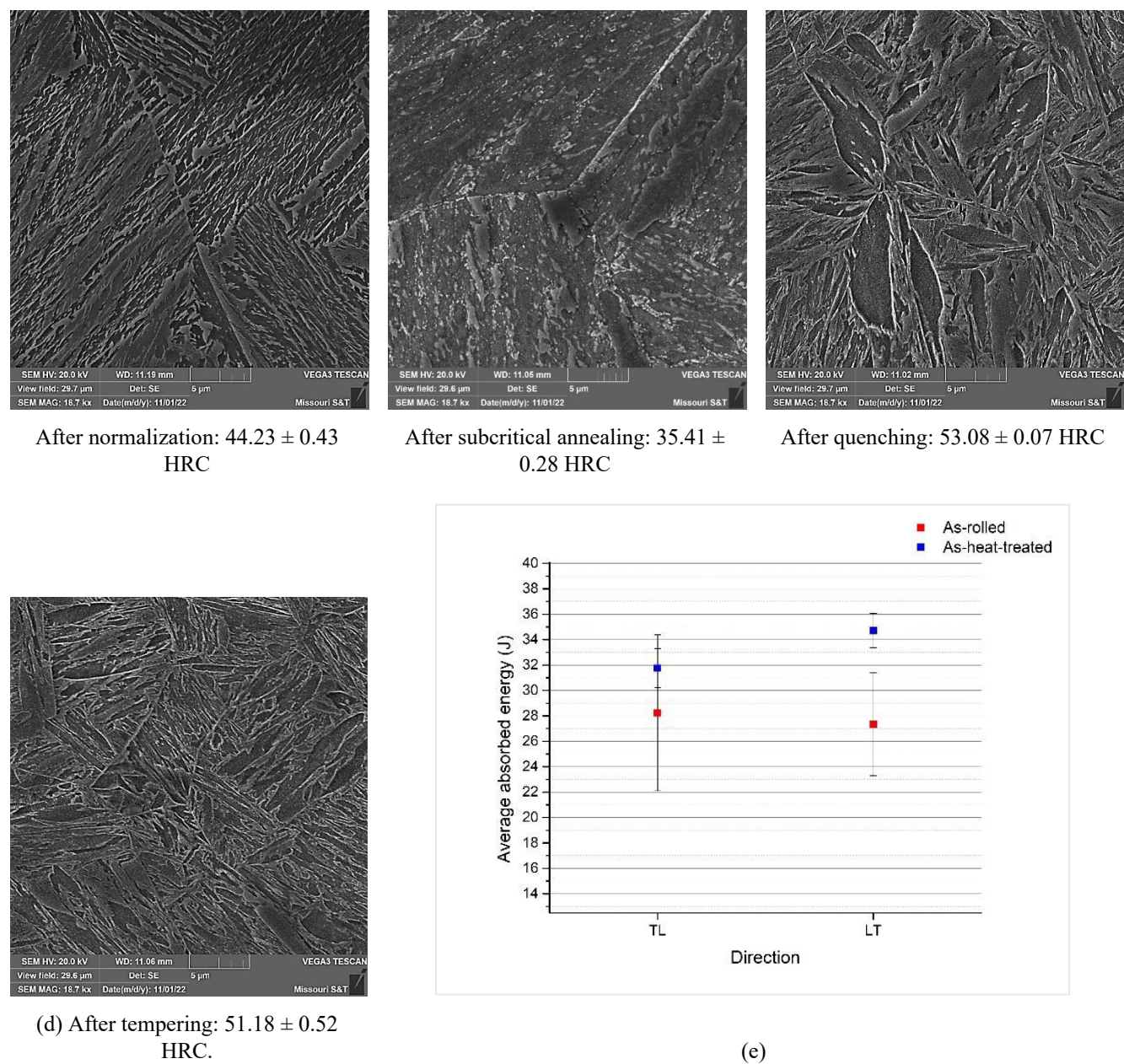


Figure 9. Reference plate results: (a)–(d): Microstructural evolution throughout the heat treatment sequence, along with the corresponding average hardness values. (e) Impact toughness results from the CVN testing in both directions Longitudinal (LT) and Transverse (TL), and in the as-rolled and after heat treatment condition.

### CONCLUSION

The findings of this study demonstrate that controlled rolling below the recrystallization temperature effectively refines the prior austenite grain size in CrNiMoV steel, significantly enhancing its hardenability. As a result, the rolled plate developed a more favorable microstructural response upon quenching, characterized by a higher fraction of martensite and a consistent transformation behavior across various cooling rates. Although the final hardness of the rolled plate after complete heat treatment was slightly lower than that of the reference plate (48.5 HRC vs. 51 HRC), its impact toughness at  $-40\text{ }^{\circ}\text{C}$  was comparably improved. This indicates a more optimal balance of strength and toughness, which is critical for structural

applications requiring both properties. Moreover, while anisotropy in toughness was observed in the rolled plate after heat treatment, the reference plate initially showed isotropic behavior due to cross-rolling; nonetheless, the rolled plate achieved ~2–3 J higher impact toughness after treatment. These results support the conclusion that thermomechanical processing combined with tailored heat treatment can be an effective strategy to improve the mechanical performance of thick-section CrNiMoV steels.

## ACKNOWLEDGEMENTS

This research was sponsored by the Army Research Office and was conducted under Cooperative Agreement Number W911NF- 20-2-0251. The views and conclusions expressed in this document are those of the authors and do not necessarily reflect the official policies, either expressed or implied, of the Army Research Office or the U.S. Government. The U.S. Government is authorized to reproduce and distribute reprints for governmental purposes, notwithstanding any copyright notation herein. The authors also gratefully acknowledge the support of the U.S. Steel Research Laboratory, particularly Dr. Thinius Natarajan, for providing access to the pilot-scale rolling mill used in this investigation.

## REFERENCES

1. M. Aguiari, M. Palombo, and C. M. Rizzo, “Performance characterization of high-strength steel and quenched and tempered steels and their joints for structural applications,” *Welding in the World*, pp. 289–300, 2020, doi: 10.1007/s40194-020-01019-6.
2. M. F. Buchely *et al.*, “Calibration of the Johnson–Cook model at high temperatures for an Ultra-High Strength CrNiMoV Steel,” *Materials Science and Engineering: A*, vol. 879, no. May, p. 145219, 2023, doi: 10.1016/j.msea.2023.145219.
3. R. O. Ritchie, “The conflicts between strength and toughness,” *Nat Mater*, vol. 10, no. 11, pp. 817–822, 2011, doi: 10.1038/nmat3115.
4. D. M. Field, J. S. Montgomery, K. R. Limmer, and K. Cho, “Heat Treatment Design to Modify the Martensite Misorientation and Obtain Superior Strength–Toughness Combinations,” *Metall Mater Trans A Phys Metall Mater Sci*, vol. 51, no. 3, pp. 1038–1043, 2020, doi: 10.1007/s11661-019-05599-x.
5. E. Shigeru and N. Naoki, “Development of Thermo-Mechanical Control Process ( TMCP ) and High Performance Steel in JFE Steel,” *JFE Technical Report*, vol. 20, no. 11, pp. 1–7, 2015, [Online]. Available: <http://www.jfe-steel.co.jp/en/research/report/020/pdf/020-02.pdf>
6. M. N. Akhtar *et al.*, “Determination of non-recrystallization temperature for niobium microalloyed steel,” *Materials*, vol. 14, no. 10, pp. 1–14, 2021, doi: 10.3390/ma14102639.